Int. J. Electrochem. Sci., 10 **(2015)** 2336 - 2354

International Journal of
ELECTROCHEMICAL
SCIENCE
www.electrochemsci.org

Determination and Generation of the Corrosion Compounds on Silver Exposed to the Atmospheres

Ye Wan[1,2,*], *Xianle Wang*[2], *Xiumei Wang*[1], *Yanbo Li*[1], *Hong Sun*[2], *Ke Zhang*[2]

[1] School of Materials Science and Engineering, Shenyang Jianzhu University, Shenyang 110168, China
[2]School of Traffic and Mechanical Engineering, Shenyang Jianzhu University, Shenyang 110168, China
[*]E-mail: ywan@sjzu.edu.cn

Received: 13 December 2014 / *Accepted:* 9 January 2015 / *Published:* 19 January 2015

The chemical compounds formed on silver, exposed at Bayuquan and Shenyang sites of China, have been studied via scanning electron microscopy, the coulometric reduction, X-ray diffraction and X-ray photoelectron spectroscopy. Corrosion of silver at Shenyang is severer than at Bayuquan. AgCl, Ag_2S and Ag_2SO_4 were the main corrosion products. Ag_2O appeared on silver at Bayuquan and nearly unnoticeable at Shenyang. The amount of AgCl on silver exposed at Bayuquan is greater than at Shenyang. Neither AgBr nor AgI was detected on silver. The amount of Ag_2S at Shenyang is 2x of that at Bayuquan.

Keywords: Silver; Atmospheric corrosion; Coulomtric reduction; Silver halide film; Silver sulfide film

1. INTRODUCTION

Silver is used widely in the fields of electronics, jewellries, optoelectronics, sensor, catalysis, battery and dental material because of its high electrical and heat conductivity, and its admirable lustrous appearance. Exactly those features which make silver so attractive for the applications are also its weakness [1]. In contrast to Au, silver is not so stable a noble metal and is prone to corrosion in the ambient atmospheres. The atmospheric environmental parameters, such as temperature, relative humidity, radiation, and the aggressive chemical species including sulfur and chloride and so on, affect corrosion of silver [1-4].

Atmospheric pollution is a serious problem over the world because of the rapid industrial growth, especially in Asia in recent years [5-6]. Air pollutants form aerosols, which form thick layers

of haze in winter [7]. For example in winters of recent years, most of areas in China were often smothered in the haze owing to anthropogenic atmospheric pollution, which is rapider and higher than expected [8]. The chemical species are the main components of atmospheric pollutants. The coarse particles of chemical species also carry substantial amounts of inorganic ions, which associated with sea salt [9].

The degradation of silver in the polluted atmospheres introduces challenges to its reliable usage. It is of fundamental interest to understand the corrosion compounds and their formation processes on the surfaces of silver at the polluted areas for the sake of reducing atmospheric attack and controlling material corrosion in the near future. However, what corrosion compounds can be formed on silver at the sites? How is the growth rates for the compounds of silver? Previous work has shown that corrosion compounds, formed due to different physical and chemical reactions on the surfaces of silver in the simulated indoor atmospheres, involved Ag_2O and AgCl [1-4, 10]. It is believed the amount of each reaction product on silver surface can be used to evaluate the cumulative pollution exposure from the environment, such as chloride [11]. The main corrosion product was AgCl and corrosion amounts for silver species increase linearly with exposure time [2]. Several reaction mechanisms of silver corrosion in the indoor atmospheres have been considered [4, 12-16]. Although no other species (except AgCl and Ag_2O) was detected on silver for the indoor exposure, a small amount of Ag_2S on silver was observed at outdoor exposure at West Jefferson, USA [2, 17], where sulfur should be at a very low level.

Atmospheric corrosion of silver at field sites has been studied sufficiently in many countries and silver databases were established on the basis of the hard data. However, most of the studies were usually devoted to the formation of silver oxides, AgCl and Ag_2S [2-4, 17]. Note that SO_2 is one of the main atmospheric pollutants in the industry areas. Therefore, it is possible there is sulfate species on the silver surface in the outdoor exposure because of SO_2 oxidation reaction [18]. In addition, the other halides except AgCl, such as bromide and iodide, are possible species in sea-salt particles in the marine atmospheres. As the anion adsorption for silver increases in the order of $I^- > Br^- > Cl^-$ [19], AgBr and AgI are the expected species on the silver exposed to the marine atmospheres as well. The corrosion behaviors of silver are still not well understood because of the complexity of environmental parameters in the outdoor atmospheres. Moreover, up to now, no detailed corrosion data of silver from outdoor exposure in China is available. In the study reported here, we exposed silver to marine and industry locations of China for up to three months and then identified the species changes in the corrosion layer that formed on the silver surfaces. It is the purpose of this paper to describe and elucidate the corrosion products and growing amounts of the corrosion compounds on the silver exposed to the two locations of China. Another goal is to enhance the understanding of species at the corrosion product/substrate interfaces by combining X-ray photoelectron spectroscopy (XPS), X-ray diffraction and coulometric reduction methods. In this way, we can also compare the pollution severity of the exposing areas.

2. EXPERIMENTAL

2.1. Specimen and electrochemical cell

Silver specimen (99.99% purity) with the size of 45 mm × 15 mm × 1 mm were wet polished with SiC paper (successively 800 and 1000 grits), degreased with alcohol and rinsed with deionized (DI) water prior to exposure experiments and electrochemical test.

2.2. Field exposures

Field exposures of silver were conducted at two geolocations of Liaoning province in China: Shenyang, an urban atmosphere and Bayuquan, a marine atmosphere. The exposure site at Bayuquan is ca. 500 m to the coastal line. Silver specimens exposed to the field sites were mounted onto plastic test cards, which were kept in a shield. The shield is transparent to sunlight and open to provide free and natural airflow around the specimen. The specimens were placed 45º to the horizon. The exposure began in June, 2012 and lasted for up to three months. The average environmental parameters in June were shown in Table 1. An ultraviolet (UV) power meter (Model FU-100†, Skyworth Science and Technology Development Co., Ltd., Beijing, China) was used to measure the UV light intensity. The concentration of ozone was recorded with an ozone analyzer (WT-80, Weitai Science & Technology Co., Ltd., Shanghai, China) generally used for monitoring ambient air.

Table 1. Average environmental parameters at the field sites through June to August.

	Shenyang	Bayuquan
Average UV light intensity, W/m^2	29.0	71.2
Average O_3 concentration, ppb	68.6	145.8
Relative Humidity (RH), %	65.4	75.5
Average temperature, ºC	20-31	25-32

2.3 Surface examination

After retrieved from the field sites, the corrosion behaviors of the exposed silver were examined with many methods. The images of the specimens were observed using a Panasonic® digital camera and scanning electron microscopy (SEM) (s-4800, Hitachi, Japan) equipped with energy-dispersive x-ray spectroscopy (EDS) modes. The structures of the specimens were identified with an X-ray diffraction (XRD) (D/max-2400, Rigaku, Japan) with Cu Kα radiation. In order to ascertain the chemical compositions and the depth distribution of the corrosion products on the surface of silver, an ex situ X-ray photoelectron spectroscopy (XPS) (an ESCALAB250, Thermo VG, USA) was employed. The details of XPS measurement were reported in the previous work [20].

2.4 Electrochemical measurement

After the exposure, the corrosion products formed on silver during the field exposure were analyzed with coulometric reduction in the 0.1 $mol \cdot L^{-1}$ sodium sulfate (Na_2SO_4) reduction electrolyte. The pH of the electrolyte was adjusted to be 10 by dropping 1 $mol \cdot L^{-1}$ sodium hydroxide (NaOH) into it. The coulometric reduction method was described in detail in the previous work [2]. The reduction potential and the reduction charge are extracted from each reduction curve. The reduction potentials serve to identify the chemical compositions of the corrosion products and were determined as the potential of the curve at the midpoint of an invariant portion of the reduction curve. The total reduction charge passed at one potential represents the amount of that compound present on the specimen. The thickness of the corrosion product layer of silver can be calculated from the reduction charge, assuming that the corrosion product film forms with theoretical density. The electrochemical experiments were performed in a three-electrode cell with an instrument (LK3200A, Lanlike Co. Ltd., Tianjin, CN) combined with an electrochemistry software named LK3200A. The cell exposed a 1 cm^2 portion of the specimen to be work electrodes. Pt wire mesh was served as the counter electrode. A saturated calomel reference electrode (SCE, + 0.244 V/NHE) was used in the sulfide, the hydrosulfide and the halide electrolytes, and a saturated mercury/mercurous sulfate reference electrode (MSE, + 0.613 V/NHE) was used in the sulfate electrolyte. The data are reported according to the electrodes used in the particular experiments. The electrolyte for cyclic voltammetry (CV) was highly basic solution to ensure that all of the sulfide being in the form of HS^- [21]. The concentration of HS^- was identified by iodimetry [22]. The solutions were flushed with nitrogen before and during the electrochemical tests. Deionized (DI) water was used throughout. All the chemicals for the electrochemical tests were Sinopharm certified. Each electrochemical experiment was repeated at least three times on different occasions and the variation in response was less than 5 mV at 25 ºC.

3. RESULTS

3.1 Surface images of corrosion layer

After the specimens were retrieved from the fields, the pictures of the surfaces were taken with a camera. Fig. 1 shows a layer of corrosion film was evident on the surfaces of the exposed specimens, which exhibited different color when different exposure periods or sites were applied. The surfaces of all the specimens appeared yellow at Bayuquan site. It is clear that the color is growing deeper as the exposure time going on at both of Shenyang and Bayuquan sites. The specimens presented dark blue color after exposed two months and developed to be dark for longer duration. Obviously, exposure generated much more corrosion products at Shenyang site than Bayuquan site, and the specimens at Shenyang site presented different characteristic from those at Bayuquan site.

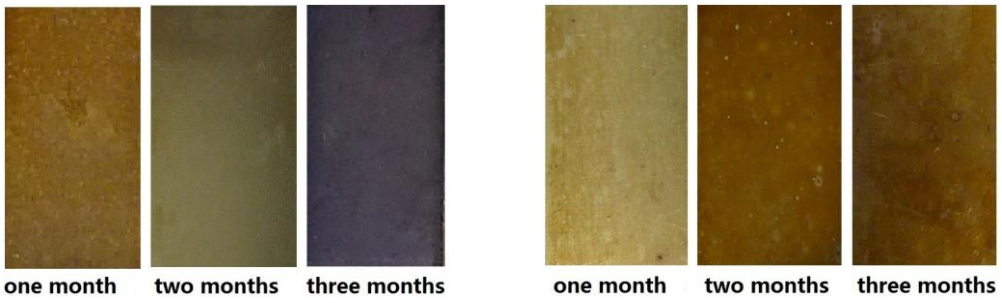

Figure 1. Surface photos of the specimen after exposure for different duration at (a) Shenyang and (b) Bayuquan sites.

The SEM images also reflected the difference in corrosion extent. SEM micrographs showing the morphologies of the exposed specimens at Shenyang site are presented in Fig. 2. It can be seen that the specimens corroded more seriously for longer exposure. The SEM micrograph of the specimen was featured by particles with the size of no more than 80 nm and covered with a uniform layer on the surface after one month exposure, which can be seen in Fig. 2a. Some particles agglomerated together and formed small clumps.

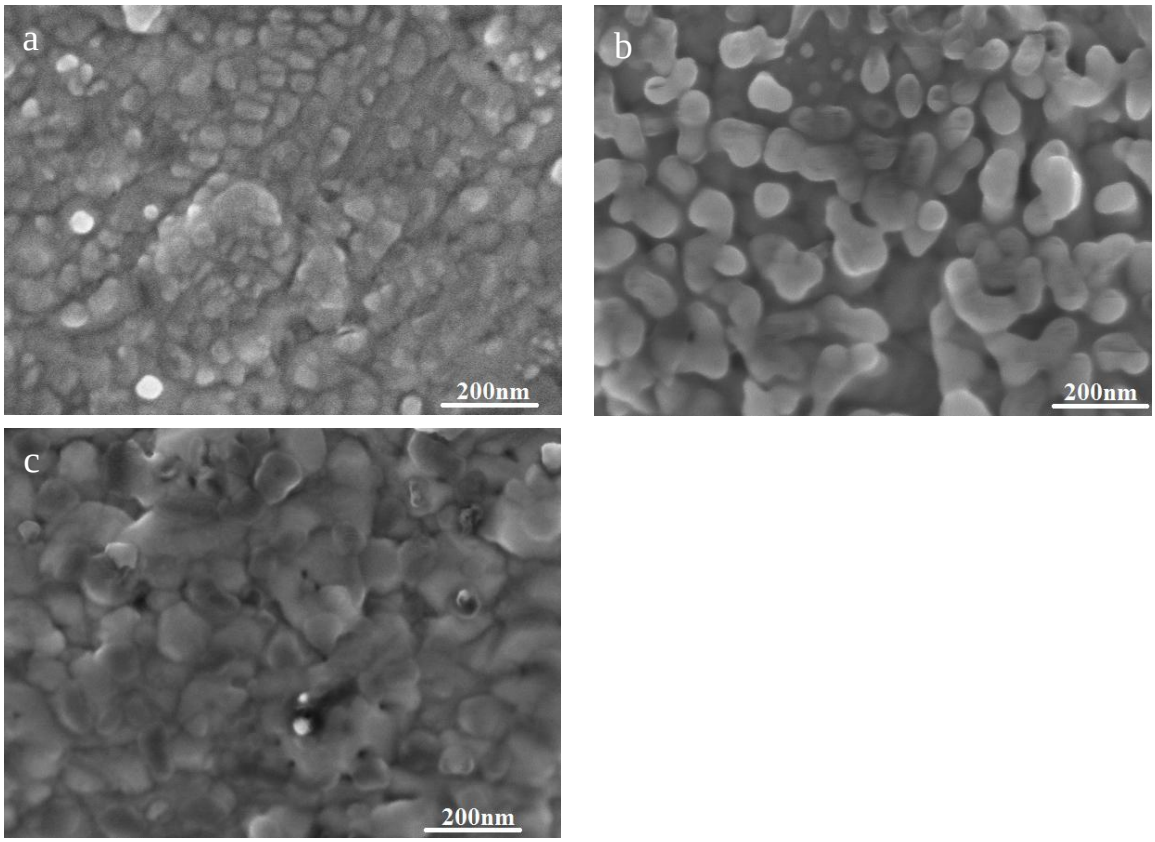

Figure 2. SEM images of the surfaces of silver exposed for different time at Shenyang site. (a) one month, (b) two months, and (c) three months.

Fig. 2 depicts layer upon layer of rounded particles expanded laterally and thickening to cover the former layer during the growth of the corrosion film over the exposure time, which demonstrated the morphological change in corrosion film evolution. The SEM images clearly show uniform corrosion occurred on silver at the field sites, although space between rounded particles can be seen in the SEM morphology. Note that the top layer was non-continuous on the specimen after two-month exposure and it grew to be a continuous layer after exposed three months, shown in Fig. 2c. The EDS results (not shown) confirm the elemental compositions of the particles involved silver, oxygen, sulfur and chloride. The contents of oxygen on the silver surfaces decreased and sulfur and chloride increased with the exposure time as well.

The SEM micrographs of the corroded surface of the specimens exposed at Bayuquan site are presented in Fig. 3.

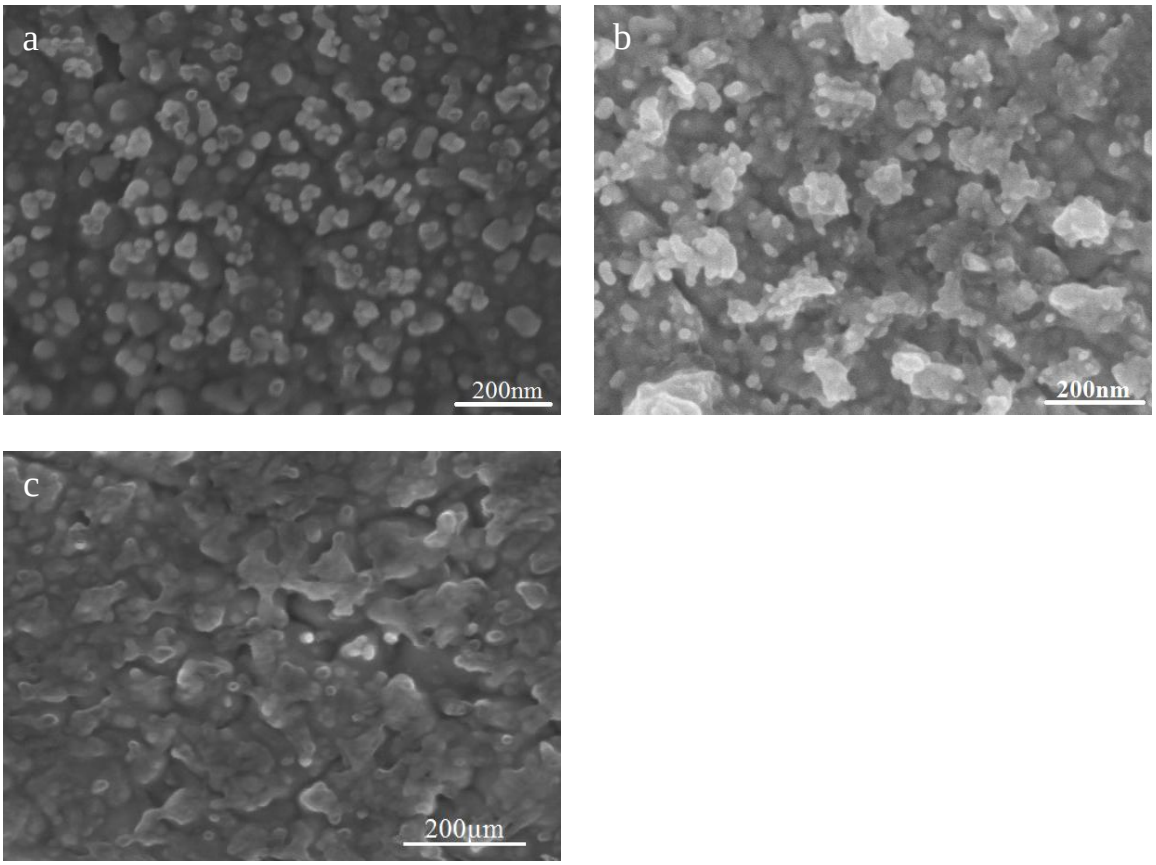

Figure 3. SEM images of the surface of the silver exposed for different time at Bayuquan site, (a) one month, (b) two months, and (c) three months.

Rounded nano crystal particles, with the size of ca. 40 nm (Fig. 3a) on silver after one-month exposure, grew on the substrate laterally and thickening to comprise corrosion product clumps on the outer corrosion layer of silver. The inner corrosion layer was denser than the outer layer. As the exposure period lengthened, the non-continuous clumps increased gradually and formed a continuous layer though spaces still can be seen, as shown in Fig. 3a, b and c. The EDS results (not shown)

confirm the elemental compositions of the particles involved silver, sulfur, chloride and oxygen and the content of oxygen decreased and sulfur and chloride increased with the exposure time.

3.2 Phase identification of corrosion compounds by XRD

In order to investigate the correlation between the results from Shenyang site and Bayuquan site, the corroded silver surface from each site were analyzed to identify the corrosion compounds of silver.

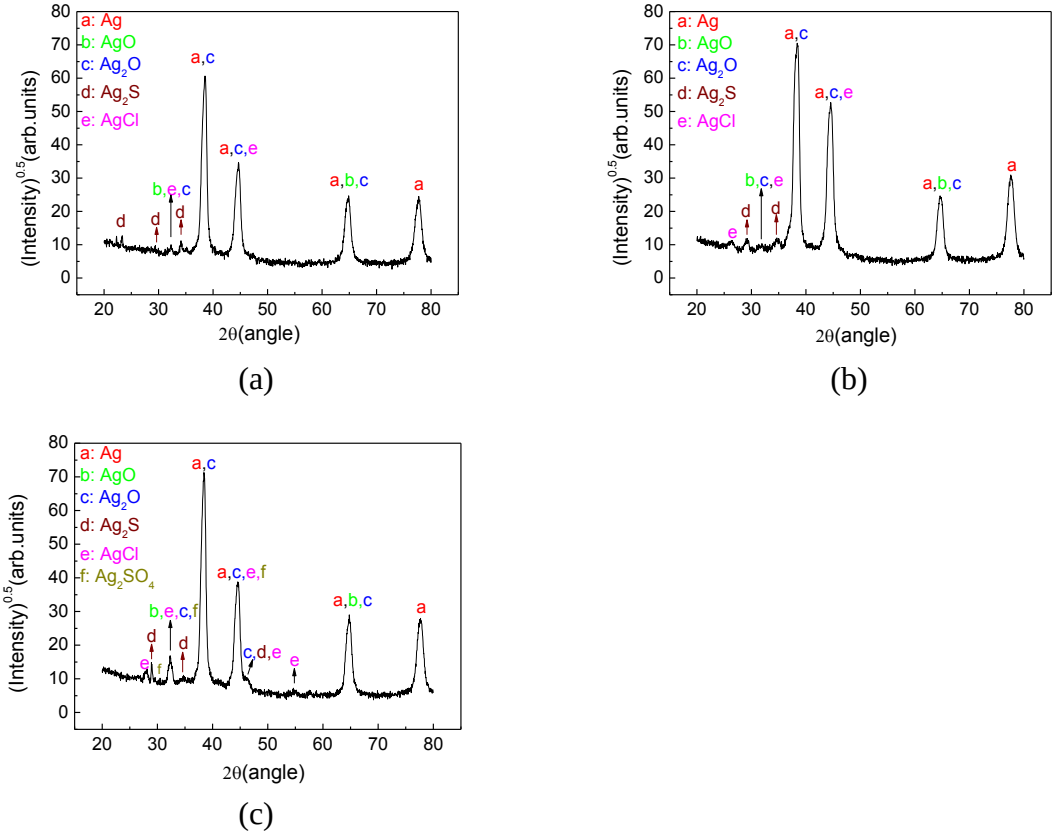

Figure 4. XRD pattern of the surfaces of the specimens exposed for (a) one month at Shenyang site, (b) three months at Shenyang site and (c) three months at Bayuquan site.

Because of the complex of the corrosion compounds and the limitations of individual techniques, a suite of complementary analytical techniques were used. The XRD patterns of the corrosion products formed on the specimens after one-month and three-month exposures at Shenyang site are shown in Fig. 4a and b respectively. Resulting diffraction patterns were analyzed and peaks were identified using Jade Software (version 6.5, Material Data Inc., California, USA). The peaks when 2θs were about 38.1°, 44.3°, 64.4°, and 77.4° belonged to the crystal faces (111), (200), (220) and (311) of metallic Ag respectively. The series of crystalline peaks were identified as the crystal

faces of AgCl when the 2θs were approximately 27.8° (111), 32.2° (200), 46.2° (220) and 57.5° (222). The peaks, 2θs were ca. 22.3°, 29°, 34.7°, 37.8°, 44.0°, 46.1° and 46.9°, were due to Ag_2S (unknown face), Ag_2S (111), Ag_2S (022), Ag_2S ($\bar{1}$03), Ag_2S (103), Ag_2S (113) and Ag_2S (004) respectively. The peaks of silver (I) oxide (Ag_2O) are known to be at 32.2° ($\bar{1}$11), 38.1° (200), and 54.8° (220), which overlap some peaks for AgCl and metallic Ag. The peak positions of silver (II) oxide (AgO) are at 32.2° ($\bar{1}$11), 37.3° (111) and 64.1° (022), which overlap some peaks for Ag_2O and metallic Ag. We can't distinguish Ag_2O, AgO, AgCl from metallic Ag by XRD and will employ other methods to help identify them in the following sections. The XRD peaks of Ag_2SO_4 were detected when 2θ=30.5º, 32.2º and 44.3º on the silver specimens after exposed three months at Bayuquan site.

Comparing Fig. 4a and b, it can be seen that the corrosion compounds of silver after one month and three months at Shenyang site were the same, although the relative intensities of the peaks of the compounds on silver surfaces were different.

3.3 Phase identification of corrosion compounds by electrochemical tests

Cyclic voltammetric tests at a rate of 10 $mV \cdot s^{-1}$ for a silver electrode were carried out to identify the reduction potential of Ag_2S. Significant potential regions, identifying the redox processes, during the formation and reduction of Ag_2S, were investigated by first performing cyclic voltammtric scanning in 0.1 $mol \cdot L^{-1}$ HS^- + 1 $mol \cdot L^{-1}$ NaOH solution in Fig. 5. The main current response to potential in Fig. 5 is in coincidence with the work by Birss et al [21] with the expected difference arising from the difference solutions. The pre-peak, labeled A_0, and the peak, labeled A_1, located at ca. -0.757 V_{SCE} (-1.126 V_{MSE}) and ca. -0.497 V_{SCE} (-0.866 V_{MSE}) respectively on the positive-going scan. The pre-peak (A_0) region has been ascribed to the formation of a monolayer of Ag_2S as a precursor to the formation of a bulk film of the phase Ag_2S on the Ag substrate [21]. Peak A_1, assigned as the formation of the bulk film, owed to the electro-formation of the phase Ag_2S under diffusion control [23]. The currents of the peaks A_0 and A_1 depend on the pH and the sulfide concentration in the solution.

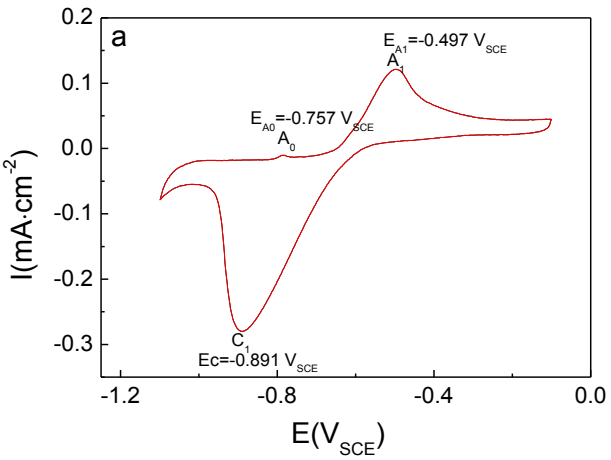

Figure 5. Volammogram ran at 10 $mV \cdot S^{-1}$ (single scan) in 0.1 $mol \cdot L^{-1}$ HS^- + 1 $mol \cdot L^{-1}$ NaOH solution.

The reduction of anodically formed Ag_2S film showed a single large peak in the cyclic voltammetric curve. The cathodic peak labeled C_1 (-0.891 V_{SCE}, -1.26 V_{MSE}), arose during the reverse scan, was due to the electro-reduction of Ag_2S. In this case, the large peak potential separation between the A_1 and C_1 peaks indicates the irreversible behavior of the system [24]. The asymmetric pairs of peaks are indicative of the low concentration of Ag^+ and the competitive adsorption/desorption of sulfide anions [25].

In addition, in order to know the exact reduction potentials of the possible corrosion compounds in the marine atmospheres in the standard reduction electrolyte, deaerated 0.1 mol·L^{-1} sodium sulfate at pH 10, many corrosion films were fabricated on silver. Silver specimen was polarized in 0.1 mol·L^{-1} Na_2S with a constant anodic current of 1.0 mA/cm^2 for 200s to form Ag_2S. Silver halides (chloride, bromide and iodide) were fabricated by applying a constant anodic current density of 1.0 mA/cm^2 different time to the silver in the corresponding chloride-containing (500s), bromide-containing (for 200s) or iodide-containing (for 400s) solution (0.1 mol L^{-1}). The generation charges are 200 mC for silver sulfide, 500 mC for AgCl, 250 mC for AgBr and 400 mC for AgI (the generation charge was calculated from the time by multiplying by the current density). The sulfide or halide solution was then removed, and the cell was rinsed and deaerated with high pure nitrogen, and the standard reduction electrolyte was introduced into the cell. The coulometric reduction used a current density of 0.1 mA/cm^2 to measure the potentials of silver sulfide and silver halide films. Fig. 6 shows the reduction curves for the established films on Ag samples in the standard reduction electrolytes.

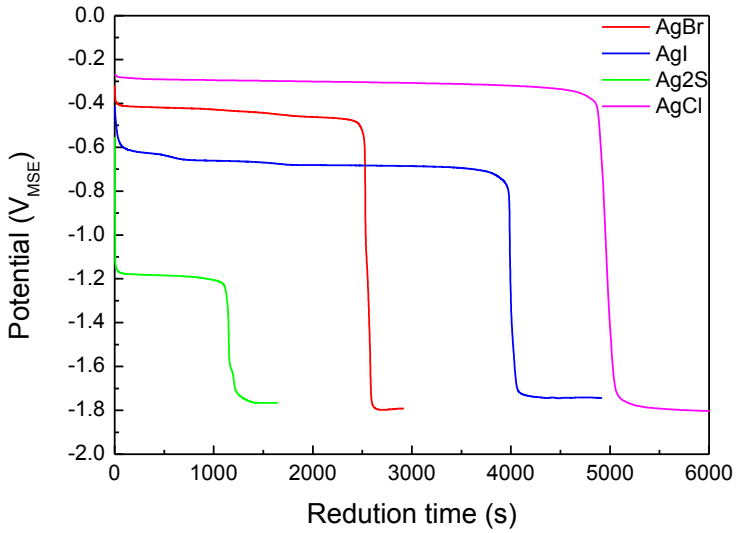

Figure 6. Reduction curves of the polarized formed films (Ag_2S, AgCl, AgBr and AgI) to show the reduction potentials of the various silver compounds investigated here. All reductions were performed in deaerated 0.1 mol·L^{-1} sodium sulfate at pH10 with a reduction current density of 0.1 mA/cm^2.

Ag_2S is shown to have a reduction potential of -1.19 V_{MSE}. Note that the potential for sulfur reduction in the standard reduction solution are different from in 0.1 mol·L^{-1} HS^- + 1 mol·L^{-1} NaOH solution, as expected because of the different solution used. The reduction potential of AgCl is ca. -

0.30 V_{MSE}, AgBr ca. - 0.412 V_{MSE} and AgI ca. - 0.673 V_{MSE} in the standard sulfate solution, which can be seen in Fig. 6. The reduction charges are approximately 115 mC, 508 mC, 255 mC and 400 mC for Ag_2S, AgCl, AgBr and AgI respectively. The generation charge of AgI equates the reduction charge of AgI, which means the efficiency of polarization process for the formation of AgI is 100%. The difference between the generation charge and reduction charge for Ag_2S, AgCl and AgBr indicate variability in the efficiency of the polarization process. For the Ag_2S case, the reduction charge was less than the generation charge. This effect could be the result of another reaction besides sulfide formation, so that the generation process was not 100% current efficient. Some of the Ag_2S might have dissolved during the generation process, or some amount of AgHS might have formed.

3.4 Corrosion amounts by coulometric reduction

After retrieved from Shenyang and Bayuquan sites, the surfaces of silver were analyzed using the coulometric reduction method with 0.1 mA/cm^2 current density in the standard reduction electrolyte to identify the corrosion compounds and quantify the amount present. As shown in Fig. 7, the reduction potential at approximately - 0.18 V_{MSE} belongs to the reduction potentials of Ag_2O [2-3, 26]. The corrosion compounds also involved Ag_2S and AgCl, whose reduction potentials are - 1.19 V_{MSE} and - 0.3 V_{MSE} respectively. It seems there is another reduction plateau (about -1.56 V_{MSE}) below Ag_2S in Fig. 7. Unluckily, we didn't identify the compound to which it belongs.

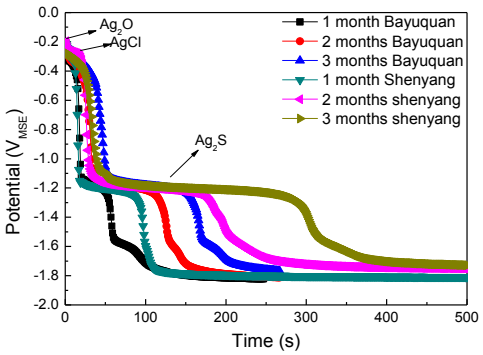

Figure 7. Coulometric reduction curves for the silver samples after exposure at Shenyang and Bayuquan sites. The reduction electrolyte was 0.1 $mol \cdot L^{-1}$ Na_2SO_4 (pH = 10) solution and deaerated 1 hour in advance. The reduction current density is - 0.1 mA/cm^2.

Reduction charges of the exposed silver were calculated from the reduction time in Fig. 7 by multiplying by the reduction current density. According to the reduction potential and the reduction time in Fig. 7, the corrosion compounds and the corresponding reduction charges for these specimens are shown in Fig. 8.

Fig. 8 shows the reduction charges of the corrosion compounds on silver exposed different time at the two field sites. The amount of all the corrosion compounds increased with the exposure time. For

all the cases, the amount of Ag_2O is small on the exposed specimens and it is higher at Bayuquan site than at Shenyang site. The amount of AgCl is higher at Bayuquan site than at Shenyang site as well and it is inverse for Ag_2S. The amount of Ag_2S at Shenyang site is ca. 2x of that at Bayuquan site.

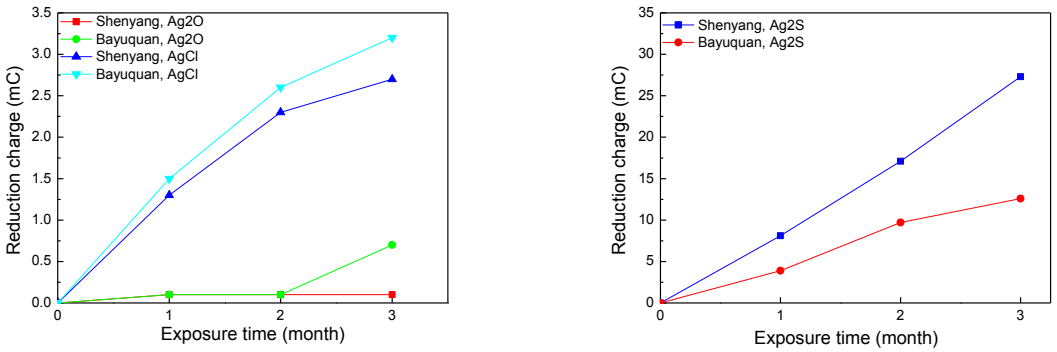

(a) (b)

Figure 8. Calculated reduction charges of the different corrosion compounds on the specimens from Fig. 7. (a) Ag_2O and AgCl, (b) Ag_2S.

3.5 Ex situ XPS study

XPS was used for further characterizing the corrosion compounds, comprised various elemental species, of the exposed silver at Shenyang site and Bayuquan site. The surfaces of the specimens were sputtered inward by XPS for 970 seconds. The XPS standard data in Fig. 9 presented the high resolution core level XPS spectra for the O 1s, S 2p, Cl 2p and Ag 3d peaks recorded after different sputtering time in an argon ion beam for the exposed silver at Shenyang site. The characteristics binding energy peaks [27] of the species and their corresponding chemicals were positioned in Fig. 9 as well. The presence of the O 1s level at ca. 531.5 eV corresponds to oxygen in the form of Ag_2SO_4, whereas the peak at 161.1 eV is consistent with S 2P in the form of Ag_2S. There are two characteristic peaks of Ag 3d observed in Fig. 9c. One was at ~368.2 eV, which is the characteristic peak of Ag $3d_{5/2}$. The other was at ~ 374.1 eV, which belongs to the characteristic peak of Ag $3d_{3/2}$. Both of them are in accordance with the characteristic peaks of Ag_2O, Ag_2S, and metallic Ag. The Cl 2p spectrum revealed that the peak at ~ 198.2 eV due to the existence of AgCl.

In an effort to corroborate distribution of corrosion compounds on silver after the exposure, sputtering depth profiles were performed by XPS. Note that the sputtering rate of XPS was almost constant during the procedure, the peak signal responses of the species as the sputtering time can be used to represent their depth profiling. Fig. 9 also depicts the compositional depth profiling by the intensities of the XPS spectra according to the sputtering time. It was found that the signals of the binding energies were dependent of depth reponses of the chemical species on the corrosion layers. The O 1s peaks observed in Fig. 9a shows the intensity of the O 1s as the function of the sputtering time. At the beginning of sputtering, the relative intensity of O 1s peak at 531.5 eV (Ag_2SO_4) is the highest and decreases as the increasing XPS sputtering depth, indicating the amount of Ag_2SO_4 is

maximum at the outmost surface and decreases toward the inner layer. Fig. 9b shows the intensities of S 2p peak at 161.1 eV (Ag_2S) at different XPS sputtering time, the relative intensity of S 2p peak is the highest at the beginning and no noticeable changes through 30s. That means there is Ag_2S in the outmost surface of the exposed silver and the amount of Ag_2S is nearly constant in 30 seconds, then the amount of Ag_2S decreased. No Ag_2S signal was recorded after 60-second sputtering. The Ag 3d XPS spectra are not so informative because Ag_2O and Ag_2S and metallic Ag don't give appreciable binding energy shift. However, the relative intensities of Ag 3d in Fig. 9c, collected from one or some of Ag_2O, Ag_2S and metallic Ag, increased with time during the sputtering. No peak of O 1s owing to Ag_2O was detected in Fig. 9a. Therefore, the increase of Ag 3d with sputtering time should be contributed to the signal response of metallic Ag. The Cl 2p signals owing to AgCl were obvious during the sputtering from the beginning to 150 s and then faded away.

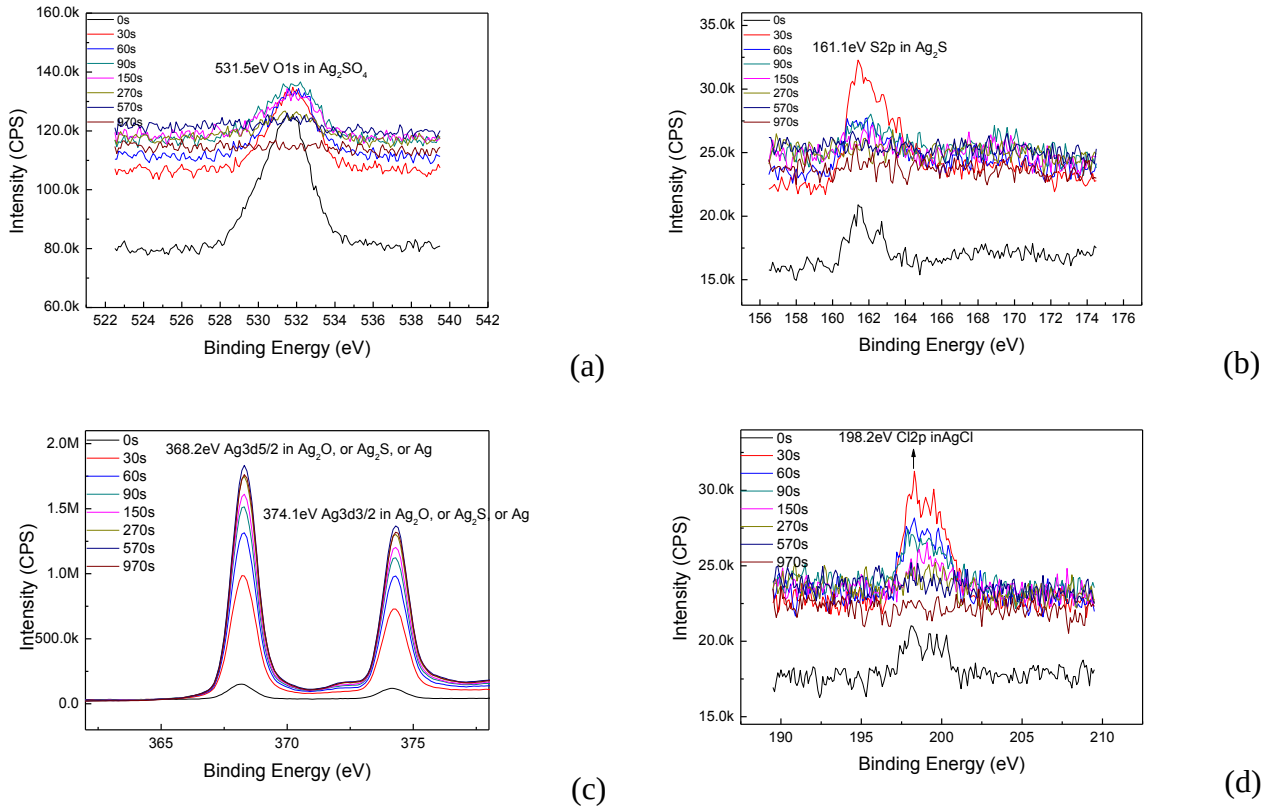

Figure 9. High resolution core level XPS spectra of the O_{1s} (a), S_{2p} (b), Ag_{3d} (c) and Cl_{2p} (d) for the specimen exposed one month at Shenyang site.

Illustrated in Fig. 10 is a series of XPS spectra acquired from the specimens, retrieved after three-month exposure at Shenyang site at different XPS sputtering time. The signal of O 1s due to Ag_2SO_4 was detected at the beginning and unnoticeable at 30 seconds sputtering (Fig. 10a). The signal of S 2p at 161.1 eV (Ag_2S) increased from the beginning to 30 s, and then it decreased with time. The S 2p signal wasn't detected at 150 seconds (Fig. 10b). Fig. 10c shows the relative intensity of Ag 3d, contributed to Ag_2S and metallic Ag, increased with the sputtering time. Note that both of Cl 2p signals at 198.2 eV and 199.6 eV, which belong to AgCl and NaCl respectively, were detected at the

beginning of sputtering (Fig. 10d). This is because NaCl deposited on the silver surface and some chloride ion was transformed to AgCl.

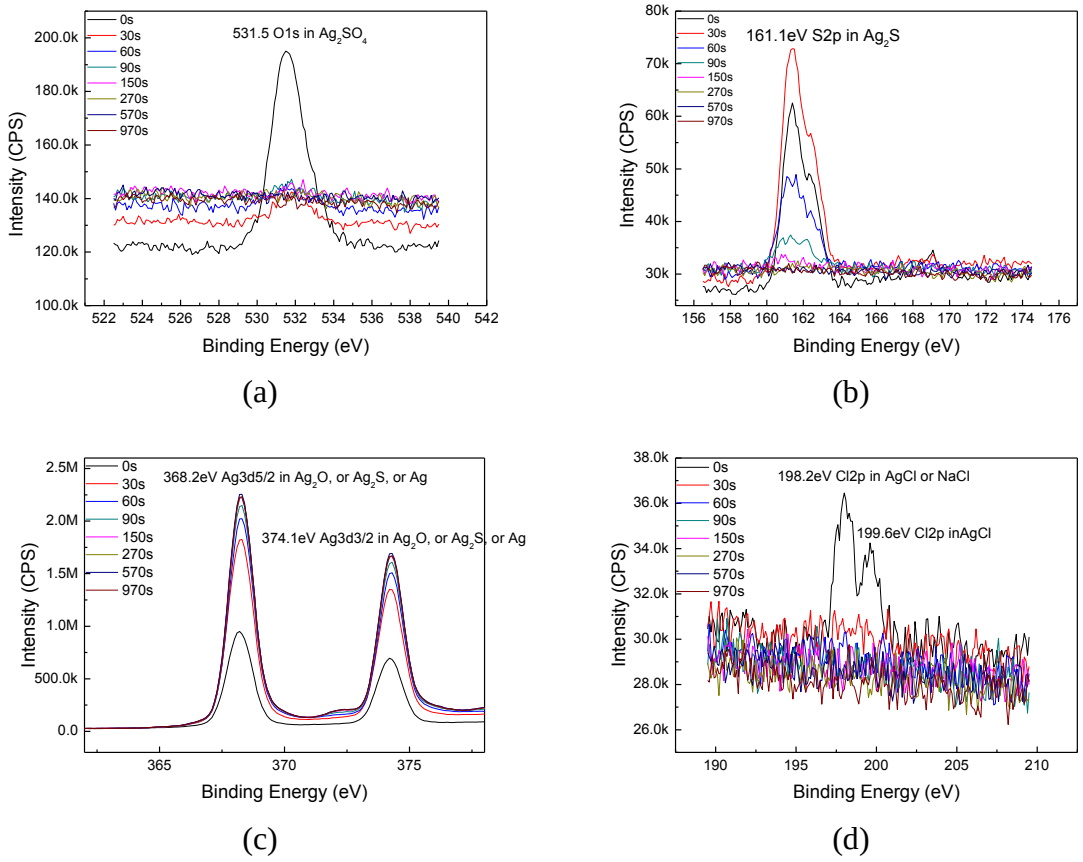

Figure 10. High resolution core level XPS spectra of the O_{1s} (a), S_{2p} (b), Cl_{2p} (c) and Ag_{3d} (d) for the specimen exposed three month at Shenyang site.

After the silver was exposed three months at Bayuquan site, the species formed on silver surface were examined in Fig. 11 as a function of the sputtering time. Fig. 11a depicts the O 1s signals owing to Ag_2O (530.9 eV) and Ag_2SO_4 (531.5 eV) can be observed. Two S 2p peaks were detected. One is at 160.7 eV, which belongs to Ag_2S. The other is at 168.4 eV, which belongs to Ag_2SO_4. The pair of Ag 3d peaks (Ag $3d_{3/2}$ and Ag $3d_{5/2}$) was due to AgO and metallic Ag. However, no O 1s peak of AgO was detected in Fig. 11a. The Ag 3d XPS signal should be contributed to metallic Ag. NaCl was detected on the outmost corrosion layer of silver at Bayuquan site as well (Fig. 11d). The relative intensities of S 2p, Ag 3d and Cl 2p varying over the sputtering time in Fig. 11 determined the formation and distribution of Ag_2S, AgCl, Ag_2SO_4 and Ag_2O on the surfaces of silver at Bayuquan site. The amount of Ag_2O, Ag_2S, AgCl and Ag_2SO_4 decreases with time throughout.

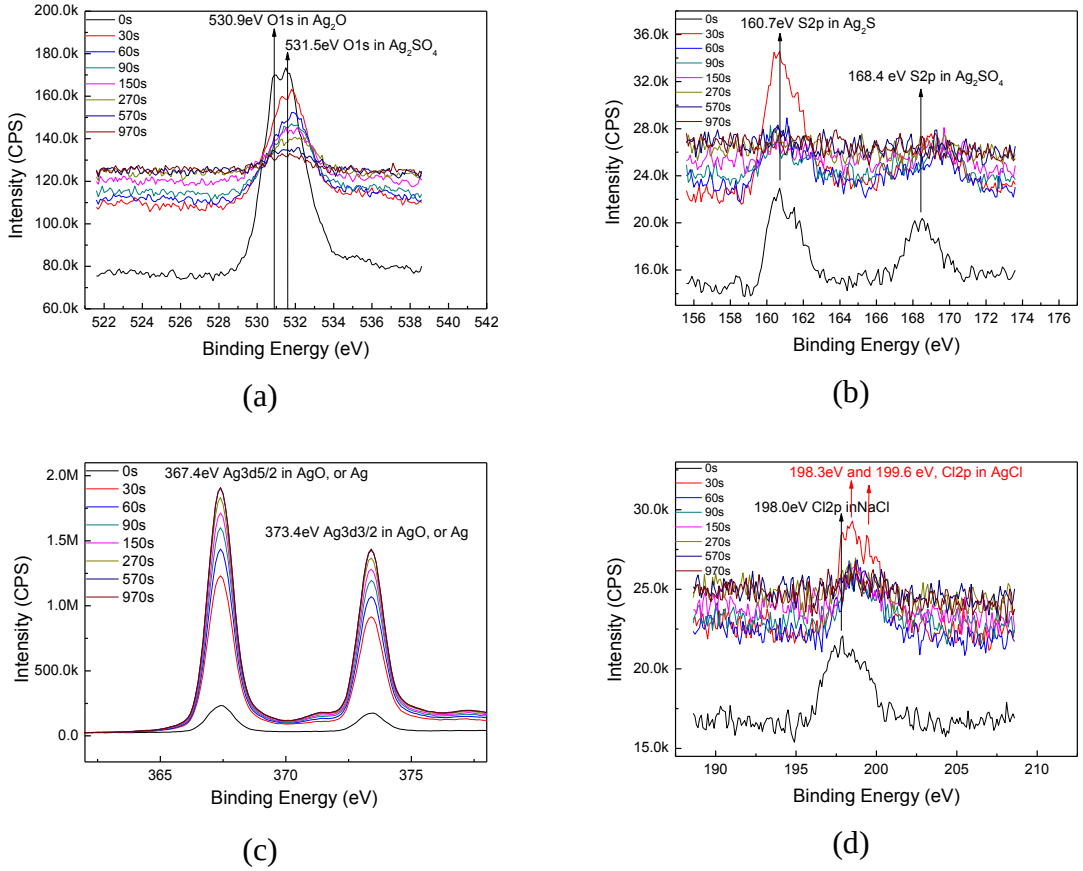

Figure 11. High resolution core level XPS spectra of the O_{1s} (a), S_{2p} (b), Ag_{3d} (c) and Cl_{2p} (d) for the specimen exposed three months at Bayuquan site.

4. DISCUSSION

Determination and growth of corrosion compounds on silver were studied after exposed at Shenyang, an industry site, and Bayuquan, a marine site. One part of the work focused on assessment of the corrosion compounds by the coulometric reduction method combined with XPS and XRD. The coulometric reduction has been used historically to evaluate insoluble solid corrosion products formed on silver and copper [16, 22, 28-30]. The reduction potentials of the established silver halides in the standard solution were recorded in order to determine the possible halide ions in the marine atmospheres, shown in Fig. 6. The reduction potential of AgCl was identified in the previous work as well [2-4]. It is interesting to note from the reduction curves of Fig. 7 that no AgBr or AgI was examined on the exposed silver even in the coastal atmosphere. Structure analysis from XRD (Fig. 4) and XPS (Fig. 9-11) also indicates that bromide and iodide are absent or so low a level in the atmospheres that can't be detected by the methods.

A small amount of Ag_2O was identified in the corrosion layer of silver at Bayuquan site by the coulometric reduction accompanied with XPS. A very small amount of silver oxides were detected on silver at Shenyang site. Previous studies reported silver oxides were mainly formed in the presence of

atomic oxygen and ozone, and UV light increased the formation of silver oxides [1-4]. The existence of Ag_2O should be from the atomic oxygen and ozone, and UV light in the marine atmospheres. The reduction potential (Fig. 7) and the XPS results revealed Ag_2S and AgCl, transformed from H_2S and NaCl respectively in the atmospheres, are important species on all the exposed silver at the two locations of China. Recall that no Ag_2S for the marine sites and a small amount of Ag_2S on the other outdoor sites was observed in America [2, 11]. The great amount of Ag_2S on the exposed silver at both of the marine site and the industry site indicated the pollution of the two atmospheres.

In addition to H_2S, the presence of SO_2 also indicated the pollution problem of the sites. Graedel [10] and Minzari et al [31] have well studied the sulfide corrosion phenomenon of silver and informed the mechanism of sulfide corrosion. Ag_2SO_4 on silver came from SO_2 in the atmospheres [31]. For all the exposed specimens in this work, no Ag_2SO_4 was detected in the corrosion film during the coulometric reduction because Ag_2SO_4 is aqueous soluble in the solution [10, 19] and transformed to Ag_2O in the alkaline reduction electrolyte. However, the results from XPS (Fig. 9-11) show the X-ray signal responses of Ag_2SO_4 on silver retrieved from the field sites.

It comes as no surprise that Ag_2S and Ag_2SO_4 are involved in the corrosion film of silver at Shenyang site because it is characterized an industry atmosphere. It is hard to believe that H_2S and SO_2 were detected in the marine atmosphere. The development of Bayuquan gives the possible reason for the results. Bayuquan is an important seaport city in China. However, the air is not as clear as before since some factories of Ansteel Group (Anshen Iron and Steel Group Corporation, China) moved to this city. Sulfur content in the atmosphere increases and this should be the reason why there was Ag_2S and Ag_2SO_4 in the corrosion film of silver in the marine atmosphere.

The other focus of this work was the corrosion amounts of silver in the two sites. Further information about the amounts of the growth process can be derived from the analysis of the coulometric reduction and the XPS signals. The results from Fig. 8 show the corrosion amounts for all the corrosion compounds on silver are greater at Shenyang than at Bayuquan for various exposure durations, which means the surface corrosion layers are thicker during the same time at Shenyang location than at Bayuquan location. The phenomenon can be seen from the color and the images of the exposed silver as well. Several interesting observations regarding the color and images of the silver surfaces at the two locations were shown in Fig. 1. The color of silver was yellow for one-month exposure and became filemot at Bayuquan location. The specimen was yellow after exposed one month and darkened after two months at Shenyang location. The denser and thicker corrosion layer was observed on silver and made its color much deeper at Shenyang than at Bayuquan (Fig. 2 and Fig. 3).

Table 1 shows both of the test sites exhibited similar temperature and relative humidity but strong variations in UV light intensity and ozone concentration. Previous work verified the vital effect of UV light intensity and ozone concentration on silver corrosion [1-4]. The atmospheric corrosion of Ag was greatly accelerated in the presence of ozone and UV light. The main environmental parameters, such as average UV light intensity, average ozone concentration and relative humidity, are lower at Shenyang than at Bayuquan. The effect of relative humidity on silver corrosion is complicated. Some researchers reported silver is susceptible to ozone oxidation at 50% RH, followed by 90% RH and 0% RH [1]. In the presence of humidity (> 60% RH) and NaCl particles on the silver

surface, the rate of silver corrosion is not strongly influenced by UV light but decreases with decreasing RH [4]. Nevertheless, the remarkable change of the corrosion rate in Fig. 8 doesn't agree with the reported effect of relative humidity because the average relative humidity is higher at Bayuquan than at Shenyang. Therefore, there must be some environmental parameters other than UV light intensity, ozone concentration and relative humidity increased greatly silver corrosion. For all the case in Fig. 8, the amount of Ag_2S is the greatest on silver specimens, which indicated sulfide corrosion being dominant on silver corrosion in both of the two sites. Based on the coulometric reduction method, we do not get the exact information of Ag_2SO_4 on the silver surface. However, the direct evidence of the involvement of SO_2 was obtained on the exposed silver in the two locations by the XPS peaks of Ag_2SO_4 in Fig. 9-11.

Ag specimens exposed at the two outdoor locations across China corroded to varying extents. Three-month exposure at Shenyang exhibited the more severe atmospheric attack than at Bayuquan. From the above discussion, the corrosion compounds involved AgCl, Ag_2S and Ag_2SO_4 on silver. Note that the corrosion rate of the corrosion compounds is indicative of the amount of the corresponding species in the atmosphere. It is reasonable that the amount of AgCl, due to chloride deposition reflecting the distance from the coastal line, in the atmosphere is greater at Bayuquan than at Shenyang (Fig. 8a) because the sea-salt deposition at marine sites is higher than at other areas. Sea-salt particles are present in air even the area is far away from the coast [12, 32-33] because of air flow. That is the reason why AgCl was detected on silver in Shenyang site as well.

The amount of Ag_2O is small and it is greater at Bayuquan than at Shenyang (Fig. 8a) for three-month exposure cases because the UV light intensity and ozone concentration at Bayuquan atmosphere is greater than at Shenyang atmosphere. As shown in Fig. 8b, the reduction charges of Ag_2S, originated from H_2S, at Shenyang site are appreciably 2x of Bayuquan for different exposure duration. This result indicated the content of H_2S at Shenyang site is much higher than at Bayuquan site. The O 1s signal at 531.5 eV, attributed to the formation of Ag_2SO_4, in the XPS depth profiles (Fig. 9a, 10a and 11a) on silver was the highest at the surface and rapidly decreased as the increasing sputtering time.

It is reported that Ag_2O and AgCl were formed at some sites and Ag_2S at other sites as well [1-4, 10]. Unfortunately, the distribution of the corrosion compounds was hardly identified because of the complex of the corrosion profiles of silver owing to the complicated atmospheres in the fields. Ex-situ XPS data (Fig. 9-11) of the film depth profiles on silver at the sites indicates unambiguously the distribution of the corrosion compounds. A summary of these reactions and the layer structures on silver exposed in the fields is given in Fig. 12 according to the XPS signal responses. The depth profiles present Ag_2S, Ag_2SO_4 and AgCl distributed on the silver surfaces at Shenyang site. The depth profiles of the chemical compounds changes drastically during the corrosion evolution of silver. Surfur ion and Chloride ion penetrated the outmost corrosion film and distributed at the film/substrate interface of silver during the one-month exposure at Shenyang. The effect of the AgCl layer, due to the retardation of the ionic transport through the layer, on limiting the corrosion of the silver substrate has been reported [34-35], which is shown in Fig. 8a that the change of the reduction charges of AgCl as exposure time exhibited decrease of corrosion rate of AgCl. For the longer exposure, sulfur ion penetrated deeper toward the substrate, while AgCl is unnoticeable at the film/substrate interface of silver after three-month exposure, shown in Fig. 12b. For the case of silver exposed three months at

Bayuquan, Ag_2S, Ag_2O, Ag_2SO_4 and AgCl was observed at the surface of silver, and Ag_2S, Ag_2O and AgCl distributed at the film/substrate interface of silver.

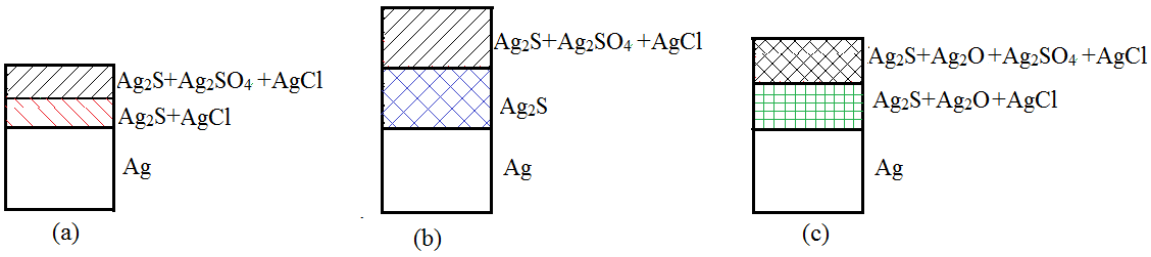

Figure 12. Scheme showing the possible corrosion layer structures on silver after exposed different time in the two sites. (a) one-month exposure at Shenyang, (b) three-month exposure at Shenyang, and (c) three-month exposure at Bayuquan.

In this respect, a comprehensive mechanism explanation is possible to be developed for the observations by considering the different reactions expected during the field exposure. From the standpoint of the layer structure, these results can be understood for a corrosion layer of different constituents where Ag_2O can greatly increase the growth of AgCl. The formation mechanism of Ag_2O in the marine atmospheres was discussed in detail in the previous studies [4]. The transformation of Ag_2O to AgCl is thermodynamically possible and induced by deposited chloride on silver. The reaction is shown in the following:

$$Ag_2O + 2Cl^- + H_2O = 2AgCl + 2OH^- \quad (1)$$

Therefore, Ag_2O, attributed to the oxidation of O_3 and atomic oxygen in the atmospheres, favors to transform to AgCl and the relative amount Ag_2O will decrease for longer exposure, which was supported by the XPS peak response in Fig. 11. The increase in the amount of Ag_2O and AgCl attack at Bayuquan is expected because O_3 concentration, UV light intensity and chloride deposition rate are bigger at Bayuquan than at Shenyang. As a result, the degrees of corrosion involving Ag_2O and AgCl are greater at Bayuquan correspondingly. The phenomenon that the amount of Ag_2S is greater at Shenyang than at Bayuquan is reasonable because Shenyang is an industry city and Bayuquan is a marine city. The great amount of Ag_2S on silver (Fig. 8b) indicated the content of S elemental is high at Bayuquan as well. This study clearly showed that atmospheric pollution is not only in the urban areas but in marine areas nowadays.

4. CONCLUSIONS

The evaluation and generation of the corrosion compounds on silver exposed to an industry site and a marine site of China were investigated by the combination of analytical techniques. The possible corrosion compounds involving silver halides and silver sulfide were established on silver by electrochemical methods to identify their reduction potentials in the standard solution. The results

show AgCl, Ag_2S, and Ag_2SO_4 were the main corrosion products on silver after exposed in the atmospheric environments. The corrosion product layers exhibited lighter color for silver at Bayuquan site than at Shenyang site. As the film thickened, the spaces between the corrosion product grains were closed and the sizes of the corrosion products grew laterally and thickening to comprise corrosion product clumps on the outer corrosion layer of silver. The XPS depth profile and the coulometric reduction analysis demonstrated that the growth of the corrosion compounds exhibited different generation amounts on silver at the two sites.

The amount of Ag_2S and AgCl, determined by the coulometric reduction and the XPS depth profile methods, increased with the exposure time for all the exposed specimens. The AgCl amount on silver exposed at Bayuquan site was greater than that of the silver at Shenyang site, which was attributed to the higher concentration of sea-salt particles in the marine atmosphere of Bayuquan. The greatest corrosion amount of the chemical species was contributed to Ag_2S in the two locations of China, which elicited H_2S concentration is high in the atmospheres and silver is sensitive to H_2S. The results also validated Shenyang is a location with higher corrosiveness than Bayuquan. Moreover, the work has revealed much about the atmospheric corrosion of silver that has previously been unobtainable in China.

ACKNOWLEDGMENTS
The authors gratefully appreciate the financial support from the National Natural Science Foundation of China (Grant Nos.: 51101106, 51131007 and 51176131) and Program for Liaoning Innovative Research Team in University (Grant No.: LT2014011).

References

1. R. Wiesinger, I. Martina and C. Kleber, M. Schreiner, *Corros. Sci*., 77 (2013) 69.
2. Y. Wan, E.N. Macha and R.G. Kelly, Modification of ASTM B117 salt spray corrosion test and its correlation to field measurements of silver corrosion, *Corros*. 68 (3) (2012) 036001-1.
3. Z.Y. Chen, D. Liang, G. Ma, G.S. Frankel, H.C. Allen and R.G. Kelly, *Corros. Eng. Sci. Technol*., 45 (2010) 169.
4. D. Liang, H.C. Allen, G.S. Frankel, Z.Y. Chen, R.G. Kelly, Y. Wu and B.E. Wyslouzil, *J. Electrochem. Soc.*, 157 (2010) C146.
5. J.H. Tan, J.C. Duan, D.H. Chen, X.H. Wang, S.J. Guo, X.H. Bi, G.Y. Sheng, K.B. He, J.M. Fu, *Atmos. Res.*, 94 (2009) 238.
6. P.D. Safai, S. Kewat, P.S. Praveen, P.S.P. Rao, G.A. Momin, K. Ali and P.C.S. Devara, *Atmos. Environ.*, 41(2007) 2699.
7. R. Gautam, N.C. Hsu, M. Kafatos and S.C. Tsay, *J. Geophys. Res.: Atmos.*, 112 (2007) 1.
8. R. Volkamer, J.L. Jimenez, F. San Martini, K. Dzepina, Q. Zhang, D. Salcedo, L.T. Molina, D.R. Worsnop and M.J. Molina, *Geophys. Res. Lett.*, 33 (2006) 1.
9. J. Lelieveld, H. Berresheim, S. Borrmann, P.J. Crutzen, F.J. Dentener, H. Fischer, and H. Ziereis, Science, 298 (2002) 794.
10. T. E. Graedel, Corrosion mechanisms for silver exposed to the atmosphere, *J. Electrochem. Soc.*, 139 (1992) 1963.
11. W.H. Abbott, A decade of corrosion monitoring in the world's military operating environments - A summary of results (Columbus, OH: Battelle Columbus Operations, 2008);

https://www.corrdefense.org/Academia Government and Industry/A Decade of Corrosion Monitoring.pdf.
12. H. Lin, G.S. Frankel, W.H. Abbott, Analysis of Ag corrosion products, *J. Electrochem. Soc.*, 160.8 (2013) C345.
13. D.W. Rice, R.J. Cappell, W. Kinsolving and J. Laskowski, *J. Electrochem. Soc.*, 127 (1980) 891.
14. S.P. Sharma, *J. Electrochem. Soc.*, 125 (1978) 2005.
15. W.E. Campbell and U.B. Thomas, *J. Electrochem. Soc.*, 76 (1939) 303.
16. Y. Fukuda, T. Fukushima, A. Sulaiman, I. Musalam, L. Yap, L. Chotimongkol, S. Judabong, A. Potjanart, O. Keowkangwal, K. Yoshihara and M. Tosa, *J. Electrochem. Soc.*, 138 (1991) 1238.
17. M. Watanabe, S. Shinozaki, E. Toyoda, K. Asakura, T. Ichino, N. Kuwaki, Y. Higashi and T. Tanaka, *Corros.*, 62 (2006) 243.
18. J.F. Meagher, E.M. Bailey and M. Luria, *J. Geophys. Res.: Oceans*, 88 (1983) 1525.
19. G.L. Richmond, H.M. Rojhantalab, J.M. Robinson and V.L. Shannon, *J. Opt. Soc. Am. B*, 4 (1987) 228.
20. Y. Wan, Y.D. Zhang, X.L. Wang and Q. Wang, *Electrochem. Commun.*, 36 (2013) 99.
21. V.I. Birss, G.A. Wright, The kinetics of the anodic formation and reduction of phase silver sulfide films on silver in aqueous sulfide solutions, *Electrochim. Acta*, 26 (1981) 1809.
22. S. Balasubramanian and V. Pugalenthi, *Water Res.*, 34.17 (2000) 4201.
23. S. Juanto, R.O. Lezna and A.J. Arvia, *Electrochim. Acta*, 39 (1994) 81.
24. E.V. Iski, M. El-Kouedi, C. Calderon, F. Wang, D.O. Bellisario, T. Ye and E.C.H. Sykes, *Electrochim. Acta*, 56 (2011) 1652.
25. J. Lee, I. Oh, S. Hwang and J. Kwak, *Langmuir*, 18 (2002) 8025.
26. ASTM B825-13, Standard Test Method for Coulometric Reduction of Surface Films on Metallic Test Samples (West Conshohocken, PA: ASTM International, 2013).
27. NIST X-ray Photoelectron Spectroscopy Database, Version 3.5 (National Institute of Standards and Technology, Gaithersburg, 2003); http://srdata.nist.gov/xps/.
28. R. B. Comizzoli, J. P. Franey, T. E. Graedel, G. W. Kammlott, A. E. Miller, A. J. Muller, G. A. Peins, L. A. Psota-Kelty, J. D. Sinclair, R. C. Wetzel and E. S. Sproles, Jr. *J. Electrochem. Soc.*, 139 (1992) 2058.
29. S. Krumbein, B. Newell and V. Pascucci, *J. Test. Eval.*, 17(1989) 357.
30. S. Lee and R.W. Staehle, *J. Electrochem. Soc.*, 142 (1995) 2189.
31. D. Minzari, M.S. Jellesen, P. Møler and R. Ambat, *Eng. Fail. Anal.*, 18 (2011) 2126.
32. I.S. Cole and D.A. Paterson, *Corros. Eng. Sci. Technol.*, 44.5 (2009) 332.
33. T. Shruti and L.H. Hihara, *J. Electrochem. Soc.*, 161 (2014) C382.
34. H. Ha and J. Payer, *Electrochim. Acta*, 56 (2011) 2781.
35. H.M. Ha and J.H. Payer, *Corros.*, 67 (2011) 046002-1.